Evidence for Channeled Diffusion of Pre-mRNAs during Nuclear RNA Transport in Metazoans

Zuzana Zachar, Joseph Kramer, Inka P. Mims, and Paul M. Bingham

Department of Biochemistry and Cell Biology, University of New York, Stony Brook, New York 11794-5215

Abstract. We report studies using an enhanced experimental system to investigate organization of nuclear pre-mRNA metabolism. It is based on the powerful genetic system and polytene nuclei of *Drosophila*. We observe (at steady state) movement of a specific pre-mRNA between its gene and the nuclear surface. This movement is isotropic, at rates consistent with diffusion and is restricted to a small nuclear subcompartment defined by exclusion from chromosome axes and the nucleolus. Bulk polyadenylated nuclear pre-mRNA precisely localizes in this same subcompartment indicating that most or all pre-mRNAs use the same route of intranuclear movement.

In addition to association with nascent transcripts, snRNPs are coconcentrated with pre-mRNA in this subcompartment. In contrast to constitutive splices, at least one regulated splice occurs slowly and may undergo execution remotely from the site of pre-mRNA synthesis. Details of our results suggest that retention of incompletely spliced pre-mRNA is a function of the nuclear surface.

We propose a simple model—based on channeled diffusion—for organization of intranuclear transport and metabolism of pre-mRNAs in polytene nuclei. We argue that this model can be generalized to all metazoan nuclei.

METAZOAN nuclei contain specific substructures implicated in pre-mRNA metabolism (see, for example, Fakan and Puvion, 1980; Lerner et al., 1981; McConnell et al., 1987; Lawrence et al., 1989; Spector, 1990; Fu and Maniatis, 1990; Carter et al., 1991; Carmo-Fonseca et al., 1991; Huang and Spector, 1991; Shermoen and O'Farrell, 1991; Wu et al., 1991; Xing and Lawrence, 1991; Li and Bingham, 1991; Kopczynski and Muskavitch, 1992). The capacity to extend these provocative observations is currently constrained by lack of a suitable genetic system for dissection of structure-function relationships and by inadequate convenience (EM) or resolution (light microscopy) among the various techniques for analysis of three dimensional organization in highly complex, compact nuclei.

We report development of a new experimental system that both augments physical analytical techniques and permits application of a powerful genetic system. Our approach exploits resources uniquely available in *Drosophila*. First, *Drosophila* has a small genome and correspondingly simple nuclear organization. Five major chromosome arms are arranged in a monolayer surrounding a single, central nucleolus (Foe and Alberts, 1985 and references therein). This allows visualization of features in diploid *Drosophila* nuclei that are obscured in larger (multilayered) diploid nuclei.

Second, in some highly polyploid nuclei all copies (up to ~500) of an individual interphase chromatid are tightly synapsed in register to produce a giant, polytene chromosome (for review see Ashburner, 1989). In contrast to most diploid interphase chromosomes, individual polytene chromosome arms are readily identifiable as discrete structures in intact nuclei. Moreover, the simple arrangement of *Drosophila* chromosome arms is retained in these giant nuclei. Thus, polytene nuclei provide an "exploded" view of a simple nucleus. Under these conditions the relatively limited resolution of rapid, convenient light microscopic techniques is sufficient to allow clear visualization of relationships between extrachromosomal features and sites of pre-mRNA synthesis.

Third, molecular genetic tools are available permitting construction of genes abundantly transcribed in polytene nuclei and producing pre-mRNAs whose processing can be experimentally regulated. This allows fluorescent in situ hybridization—a technique providing relatively high resolution, but low sensitivity—to be used to investigate organization of genetically manipulable, regulated and constitutive RNA processing events in the opportune environment of the polytene nucleus.

This experimental system permits analysis of intranuclear organization of pre-mRNA processing with unprecedented sensitivity and topological detail. Comparison of results from this enhanced system with earlier studies in more complex nuclei suggests a simple, general model for the organization of many features of metazoan pre-mRNA metabolism.

Please address all correspondence to Paul Bingham, Department of Biochemistry and Cell Biology, University of New York, Stony Brook, NY 11794-5215.

Materials and Methods

Structure of the SgSLAC1 Chimeric Gene

SgSLAC1 (Fig. 1, *bottom panel*) consists of the following segment inserted in the *SalI* polylinker site in the Carnegie-20 germline gene transfer vector (Rubin and Spradling, 1983) in the opposite transcriptional orientation to the *rosy* gene marking the vector. The *Sgs-4* promoter segment (from the *pCl.9* plasmid of McNabb and Beckendorf [1986]) extends from a synthetic *SalI* site ca. 850 bases 5′ to the transcription start site through the *HindIII* site 740 bases 3′ to the start. This is followed by the *suppressor-of-white-apricot* (*su(w^a)*) segment extending from an *AvaII* site in the first exon (coordinate 767 [Chou et al., 1987*b*]) through the *HincII* site in the fourth exon (coordinate 3,502). (A small segment of the first intron [coordinate 842 through 1,200] has been deleted. This has little or no effect on splicing and regulation of the first *su(w^a)* intron [Mims, I. P., and P. M. Bingham, unpublished observations].) This is followed by the LacZ gene and SV40 polyadenylation signal described by Thummel et al. (1988). This is followed by the 3′ nontranscribed segment from *su(w^a)* extending from the *SstI* site at coordinate 5,857 through the *XhoI* site ca. 2 kb off the 3′ end of the sequenced interval (Chou et al., 1987*b*).

Fly Strains and Genetic Manipulation

Most fly strains used have been described previously (Li and Bingham, 1991; Zachar et al., 1987; Lindsley and Zimm, 1992). The *su(w^a)* deletion strain is the g165 gamma-ray-induced mutant allele. This deficiency removes a segment beginning in the second *su(w^a)* intron and extending 5′ through and beyond the *su(w^a)* promoter region. This allele behaves as a null for *su(w^a)* function. Low levels of transcripts promoted from an unknown upstream start and extending through at least the central portion of the remaining *su(w^a)* segments are produced by this allele (our unpublished observations; see Fig. 5 *D*).

SgSLAC1 was introduced into our standard *ry cn* [*su(w^a)*] double mutant strain by conventional germline gene transfer methods (Rubin and Spradling, 1983; Chou et al., 1987*a*). All experiments described were carried out in the *su(w^a)*$^+$ background except where otherwise indicated. To examine SgSLAC1 expression in the absence of the *su(w^a)* protein SgSLAC1 was introgressed into a genetic background containing the *su(w^a)^{g165}* deletion allele (above). Each of two independent SgSLAC1 insertions behaved indistinguishably as assessed by Northern and in situ hybridization analysis.

Probe Synthesis

Biotinylated and digoxygenylated RNA probes were synthesized on linearized DNA templates with SP6, T3, or T7 polymerase using conventional procedures (Krieg and Melton, 1987; Boehringer-Mannheim product description). Biotinylated (Sigma Chem. Co., St. Louis, MO) or digoxygenylated (Boehringer Mannheim Corp., Indianapolis, IN) UTP was used at 3.3 mM in combination with 6.7 mM nonderivatized UTP.

Radioactive probes for Northern and S_1 protection analyses were conventional riboprobes (Krieg and Melton, 1987).

In situ hybridization probes were degraded to an average length of 75–150 bases (Cox et al., 1984). Probe segments used are as follows: Intron 1, intron 2, exon 4, and 3′ probes (Figs. 1 and 4) are derived from *su(w^a)* sequences 1,200 through 1,640, 2,023 through 2,667, 2,840 through 3,502, and 5,857 through the Xho I site ca. 2 kb 3′ to the end of the sequenced *su(w^a)* interval (coordinates and sequence according to Chou et al., 1987*b*). LacZ, control, and exon 5 probes (Figs. 1–4 and 6–8) are derived from plasmid *pC4beta-gal* carrying LacZ followed by the SV40 polyadenylation signal (Thummel et al., 1988) and are as follows: LacZ probe is a 3.4-kb segment from the polylinker *Eco RI* to the *XbaI* site at the 3′ end of LacZ; control is the ca. 600 base *AvaI–SstI* segment from the central portion of LacZ and exon 5 is the ca. 850 base *XbaI–EcoRI* SV40 segment. The *Sgs-4* probe (Fig. 6, *I–K*) (derived from plasmid *pCl.9* [McNabb and Beckendorf, 1986]) is the 780 base *EcoRI–HindIII* fragment covering most of the *Sgs-4* transcription unit. The *rosy* probe (Fig. 2, O–R) (derived from Carnegie-20 [Rubin and Spradling, 1983]) is the 4.0-kb *HindIII–EcoRI* fragment containing the 3′ portion of the *rosy* transcription unit.

The *Drosophila* snRNA hybridization probes (U1, U2, U4, U5, and U6) are described by Spikes and Bingham (1992). Each probe is homologous to most or all of the corresponding snRNA.

The poly-T probe was ~60 bases in length. It was made by terminal transferase addition of digoxygenylated deoxyuridine (Boehringer Mannheim Corp.) to a 55 base long synthetic thymidylate polymer using manufacturers recommended conditions (Sigma Chem. Co.).

S_1 protection probes were as follows (Fig. 5). Probe A was a 285 base RNA containing the *su(w^a)* segment from 1,386 to 790 (with deletion of 842 through 1,200, above) with a 46 base 5′ vector extension. Probe B was a 294 base RNA consisting of the 218 base *su(w^a)* segment from 2,023 to 1,805 with a 76 base 5′ vector extension. Probe C was a 713 base RNA containing the 637 *su(w^a)* segment from 2,023 through 1,386 with a 76 base 5′ vector extension. Probe D was a 1,345 base RNA containing the 1,107 base *su(w^a)* fragment from coordinate 3,502 through 2,395 plus a 32 base 5′ and 206 base 3′ extension consisting of surrounding vector sequences. The *Sgs-4* probe was the 409 base RNA consisting of 345 base *Sgs-4 HindIII–BalI* fragment covering the 3′ end/polyadenylation signal (McNabb and Beckendorf, 1986) with a 64 base 5′ vector extension. The U2 snRNA protection probe was a 291 base RNA consisting of a 192 base U2-homologous segment with a 73 base 5′ and 26 base 3′ vector extension (Spikes and Bingham, 1992).

Tissue Preparation

Tissue was prepared by cryosectioning late (migratory) third instar larvae in OCT mounting medium. 28 μm sections were used unless otherwise indicated. Sections were immediately fixed in 3.7% formaldehyde in PBS (formaldehyde/PBS) for 10 min, and then washed in PBS.

Tissue "smears" were used in place of sections as indicated. These were prepared by dissecting larval tissues in PBS, fixing for 1 min in formaldehyde/PBS, gently smearing between coverslip and slide (to break most cells but not most nuclei), fixing an additional 1 min, flipping off the coverslip and fixing for 10 additional min in formaldehyde/PBS, and washing in PBS. Smears produce some flattening and stretching of nuclei; however, essential structural features relevant to this study are largely or entirely preserved.

Cleaned, polylysine-coated slides were used throughout and prepared according to polylysine manufacturer's instructions (Sigma Chem. Co.).

Immunolocalization of constitutive splicing epitopes was carried out under various fixation conditions including formaldehyde/PBS, formaldehyde/PBS plus 0.1% glutaraldehyde, ethanol, methanol, and acetone. (Organic solvent fixations were carried out for 10–30 min at room temperature followed by PBS wash and subsequent processing as for formaldehyde/PBS fixation.) All conditions produce very similar or identical patterns (results not shown) indicating that the structures described are not artificial products of fixation.

In Situ Hybridization

In preparation for hybridization, sections or smears were proteolyzed, refixed, and acetylated as described (Hafen and Levine, 1986; Springer et al., 1991). Hybridization was carried out for 12–16 h in the hybridization solution described by Springer et al. (1991) at 55°C. In cases where especially low backgrounds were required (Fig. 2), slides were pretreated under hybridization conditions without probe for 1–3 h. Slides were postwashed as described in 2× SSC, 50% formamide (Springer et al., 1991).

Hybridization with poly-T was carried out as for RNA probes except that the temperature for hybridization and postwash was reduced to 37°C and 5× SSC, and 34% formamide was used as postwash solvent. For double-label hybridization to pre-mRNA and poly-A, both probes were present in the hybridization solution. These were incubated for ca. 5 h at 55°C to allow RNA probe hybridization, and then 12–16 h at 37°C to allow poly-T hybridization. Double-label hybridizations were postwashed as for poly-T hybridizations.

To prevent crushing of thick structures in cryosections, two coverslips were placed around the tissue to prop the third coverslip used to cover the sample and hybridization solution. Coverslips were sealed with rubber cement and the slides were incubated in sealed, humidified chambers.

Double-Label Hybridization to Pre-mRNA and Chromosomal DNA

Cryosections were fixed in 95% ethanol for 30 min and rehydrated in PBS. Sections were denatured by treatment in 0.1 M NaCl; 10 mM MOPS, pH 7.0, 70% formamide at 70°C for 2 min followed by 2 min under the same conditions with addition of formaldehyde to 3.7%. Sections were then PBS washed and treated as above for hybridization.

If sections were fixed directly in formaldehyde/PBS (after initial ethanol

1. *Abbreviations used in this paper*: ECN, extrachromosomal channel network; *su(w^a)*, *suppressor-of-white-apricot*.

fixation) without denaturation, pre-mRNA signals were unaffected but no DNA hybridization was detected (results not shown).

For RNase controls (Fig. 2, *N* and *R*), the denatured sections were treated with 10 μg per ml of RNaseA in 2× SSC at 37°C for 1 h, followed by exhaustive 2× SSC wash, followed by refixation in formaldehyde/PBS.

Immunolocalization

For immunolocalization of RNA probes, sections were blocked in 5% powdered non-fat dry milk in PBS (milk/PBS) for 30 min, antibody was administered for 30 min in milk/PBS, slides were washed in four changes of PBS totaling 30 min, and mounted for examination in 0.2 M Tris, pH 8.6, 60% glycerol, and 1 mg/ml of *p*-phenylenediamine (Sigma Chem. Co.).

Fluorochrome-conjugated anti-digoxygenin Fab fragments were purchased from Boehringer Mannheim Corp. Antibiotin mouse mAbs conjugated with an unusually bright, rhodamine-like fluor (Cy3) was a gift from Jackson ImmunoResearch Laboratories. These antibodies allow approximately tenfold higher signal strength with biotinylated sequence probes than conventional biotin detection systems in our hands.

Immunolocalization of various splicing-associated epitopes (antibodies described in Li and Bingham, 1991) was carried out as described for immunolocalization of biotin and digoxygenin above.

Samples were photographed under conventional epifluorescent illumination with TMax-100 film. Negatives were produced from digitalized confocal images by SlideImagers, Inc. (Atlanta, GA).

Confocal Microscopy

All confocal images were collected on an Odyssey slit scanner (Noran Instrs., Inc., Middleton, WI). For double-label detection of DNA and the B″ snRNP epitope (Fig. 7, *A* and *B*), sections were RNased and refixed as described above to destroy the RNA component of propydium iodide staining. Sections were treated with primary and secondary (fluorescein-conjugated) antibodies to visualize B″, and then stained with a dilute propydium iodide solution to produce a level of chromosomal staining (visualized through rhodamine filter sets) comparable to the intensity of fluorescein labeling of B″.

Northern and S_1 Protection Analyses

Northern analyses used polyadenylated RNAs fractionated on oligo-dT cellulose, run on formaldehyde agarose gels, and hybridized according to conventional procedures (Maniatis et al., 1982).

Total third instar nucleic acids were prepared according to Puissant and Houdebine (1990) except that the lithium chloride extraction was omitted. For fractionation into polyadenylated and nonpolyadenylated RNAs, the preparation was treated at 85–90°C for 2 min in 150 μl per 100 mg starting tissue of 1 mM Tris (pH 8.0), 0.1 mM EDTA, diluted into 450 μl of ice cold high salt buffer (10 mM Tris, pH 7.5, 1 mM EDTA, 660 mM NaCl) and made 0.5% in SDS. The RNA was passed four times over an oligo-dT cellulose column (0.5 ml bed volume per 100 mg of starting larval tissue). The material flowing through the last column pass and the first 0.6 ml wash (0.5 ml column) with binding buffer (10 mM Tris, pH 7.5, 1 mM EDTA, 500 mM NaCl, 0.5% SDS) was retained as nonpolyadenylated (flow-through) RNA. The column was then washed with two column volumes of binding buffer and bound (polyadenylated) RNA was eluted with two column volumes of 1 mM Tris, pH 7.5, 0.1 mM EDTA.

S_1 protection was carried out as follows. Ethanol precipitated larval RNA (40 mg tissue-equivalent of either flow-through or polyadenylated RNA) was resuspended in 22.5 μl of 75% formamide, 20 mM MOPS (pH 7.0), 5 mM sodium acetate, 0.1 mM EDTA, 1% SDS. Probe (ca. 10^6 dpm) and NaCl (to 400 mM) were added and hybridizations were incubated 12–18 h at 50°C. Hybridization reactions were ethanol precipitated by addition of 180 μl of 100 mM Tris (pH 8), 10 mM EDTA, 1% Sarcosyl, 1 ml ethanol, and incubation for 1 h at 0°C. Recovered pellets were dissolved in 112.5 μl of 1 mM Tris (pH 7.5), 0.1 mM EDTA. 12.5 μl of 10× S_1 buffer (300 mM sodium acetate, pH 4.6, 500 mM NaCl, 10 mM zinc acetate, 50% glycerol) and 350 U of S_1 nuclease (GIBCO BRL, Gaithersburg, MD) were added and the reaction was incubated for 15 min at 37°C. Reactions were terminated by addition of 125 μl 200 mM Tris (pH 8.0), 20 mM EDTA and 2% Sarkosyl, and extracted once with phenol/chloroform. After addition of 3 μg of yeast tRNA carrier (Sigma Chem. Co.), samples were precipitated for gel electrophoresis by addition of 5 vol 90% ethanol, 100 mM sodium acetate (pH 9.0).

Under these conditions chromosomal DNA makes no detectable contributions to the S_1 protection patterns observed (Fig. 5 and results not shown). Probes were present in substantial excess. Quantitation of relative levels of S_1 protection products (Fig. 5) was always based on comparisons of stoichiometries (autoradiographic intensities corrected for size and base composition of uniformly labeled products) of bands within the same gel channel.

Results

The Experimental System

su(w^a) is one of several genetically manipulable splicing regulators in *Drosophila* (for review see Bingham et al., 1988; Baker, 1989; Maniatis, 1991). *su(w^a)* expression is autoregulated. In the absence of *su(w^a)* protein, the *su(w^a)* pre-mRNA is spliced to produce functional mRNA. In the presence of sufficient protein levels, splicing of the first two *su(w^a)* introns is inhibited—reducing production of mRNA and resulting in accumulation of unspliced RNAs (Chou et al., 1987*b*; Zachar et al., 1987). At steady state, this feedback loop produces a mixture of spliced and incompletely spliced *su(w^a)* RNAs. The first *su(w^a)* intron is more efficiently regulated than the second.

We constructed a hybrid gene, SgSLAC1 (Fig. 1, *bottom panel*), with the following features. First, SgSLAC1 is driven by the strong *Sgs-4* promoter producing high levels of transcription in polytene salivary gland nuclei. Fused to

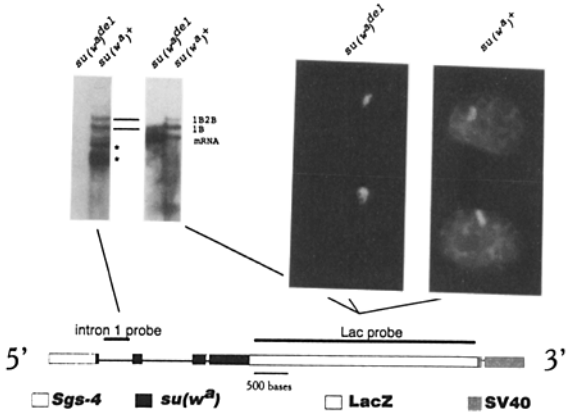

Figure 1. Structure, regulation, and salivary gland nuclear distribution of SgSLAC1 transcripts. At bottom is structure of SgSLAC1 primary transcript (exons are boxes, intron are lines). *Sgs-4*, *su(w^a)*, LacZ, and SV40 segments are indicated (Materials and Methods) as are the placement of sequence probes. Upper left is Northern analysis of polyadenylated RNA samples from third instar larvae carrying the same SgSLAC1 insertion in either the presence (+) or absence (*del*) of endogenous *su(w^a)* protein. Fully spliced SgSLAC1 mRNA or transcripts retaining the first (*1B*) or first and second introns (*1B2B*) are indicated. 1B and 1B2B transcripts from the endogenous *su(w^a)* locus are indicated by asterisks. (Note that endogenous *su(w^a)* transcripts from the entire larva are comparable within severalfold in amount to SgSLAC1 RNA produced exclusively in salivary glands. Moreover, a very disproportionately large fraction of endogenous *su(w^a)* RNA comes from nonsalivary gland [imaginal disc; our unpublished results] tissue. Thus, endogenous *su(w^a)* salivary gland transcript levels are very low and not detectable in the in situ hybridization experiments described in Fig. 4). Upper right shows representative in situ hybridizations to polytene salivary gland nuclei carrying the same SgSLAC1 insertion in either the presence (+) or absence (*del*) of the endogenous *su(w^a)* protein.

Sgs-4 is a segment containing the first three introns of the *su(w^a)* gene, followed by the LacZ gene, and followed by the polyadenylation signal from the SV40 early transcription unit. *Sgs-4*, *su(w^a)*, and LacZ protein coding sequences are joined in frame. SgSLAC1 produces salivary gland-specific beta-galactosidase by conventional histochemical assays (results not shown) demonstrating production of functional mRNA.

Second, the *Sgs-4* promoter is expressed at relatively constant levels throughout late third larval instar (McNabb and Beckendorf, 1986 and references therein) resulting in highly reproducible transcript distribution patterns at or near steady state in our experiments.

Third, the LacZ-SV40 3′ portion results in production of a relatively unstable cytoplasmic polyadenylated mRNA (Thummel et al., 1988; our unpublished results). Thus, steady state cytoplasmic SgSLAC1 mRNA levels are relatively low and do not interfere with visualization of nuclear

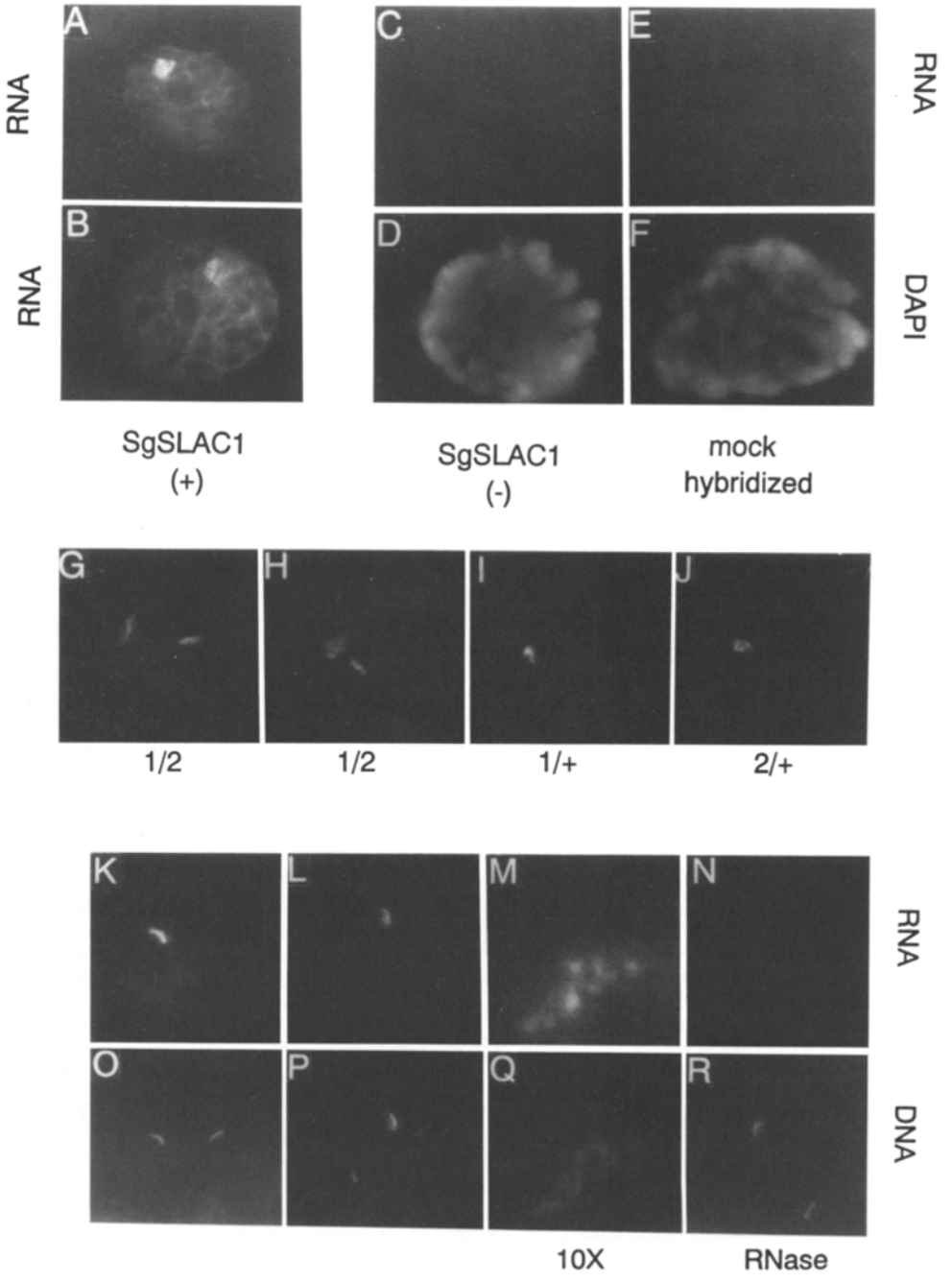

Figure 2. Primary zone pre-mRNA concentrations are intimately associated with template DNA. (*Top*) Authentication of fluorescent in situ hybridization signals. Nuclei are from smears (Materials and Methods). *A* and *B* show hybridization to pre-mRNA (*Lac*) in nuclei from an SgSLAC1-carrying strain. *C* and *D* are pre-mRNA in situ hybridization (*Lac*) and DNA (*DAPI*) signals for a nucleus from a strain lacking the SgSLAC1 construction. *E* and *F* are in situ hybridization and DNA signals after exposure of SgSLAC1-bearing nucleus to probe solution lacking RNA probe and processing through antibody visualization. (*Middle*) *G* and *H* show in situ hybridization with Lac to nuclear pre-mRNAs in larvae heterozygous for each of two independent, SgSLAC1 insertions (*1* and *2*). Control nuclei from individuals heterozygous for each SgSLAC1 insertion alone are shown in *I* and *J*. (*Bottom*) Double-label hybridization to pre-mRNA (Lac; *K–N*) and DNA (*rosy*; *Q–R*). *rosy* is ca. 2 kb 5′ to the SgSLAC1 transcription unit on the gene transfer construction. The endogenous *rosy* locus can be seen as a second labeling site in the DNA images. *M* and *Q* show the pre-mRNA and DNA labeling pattern of a primary zone approximately tenfold magnified relative to the other images. Note that the DNA and pre-mRNA signals show differences in relative local labeling intensities but are otherwise superposable. *N* and *R* show results of RNase treatment of tissue before hybridization (Materials and Methods). (Hybridization to mRNA-synonymous DNA strands by the "RNA" probe generates a signal too weak to detect under the conditions of the experiment.) Experiments in *G–R* were done in *su(w^a)^{gl65}* background to reduce ECN labeling (*text*).

pre-mRNA. These cytoplasmic mRNAs are detectable by autoradiographic in situ hybridization (results not shown) but generally not by fluorescent in situ hybridization.

Fourth, the endogenous *su(w^a)* gene is expressed in salivary gland cells. Splicing of the first two *su(w^a)* introns in SgSLAC1 is repressed by wild-type *su(w^a)* protein provided in trans indicating that these introns retain regulatability and show controlled splicing similarly to the endogenous gene (Fig. 1, *upper left*). Endogenous *su(w^a)* gene salivary gland transcript levels are too low to detect in situ hybridization experiments described here (legend to Fig. 1 and results not shown).

The Highest Concentration of SgSLAC1 Nuclear Pre-mRNAs Occurs in Intimate Association with Template DNA

We examined the subnuclear distribution of SgSLAC1 pre-mRNAs by fluorescent in situ hybridization. Control experiments demonstrate that fluorescent signals result exclusively from hybridization to SgSLAC1 RNAs. Specifically, signals depend on the presence of the SgSLAC1 gene (Fig. 2, *A–D*) and labeled RNA probe (Fig. 2, *E* and *F*). Furthermore, pretreatment of tissue with RNase (Fig. 2, *N* and *R*) or use of an mRNA synonymous probe (results not shown) eliminates the fluorescent signal.

SgSLAC1 intron and exon sequences are most concentrated in a small area we designate the primary zone—visible as the small, most brightly fluorescent region in all labeled nuclei (see for example, Fig. 2, *A* and *B* and Fig. 3). Two lines of evidence demonstrate that primary zones are concentrations of transcripts intimately associated with the transcribing gene. First, introduction of SgSLAC1 insertions at two independent chromosomal locations results in two distinct primary zones (Fig. 2, *G* and *H*). Second, double-label hybridization shows that template DNA and primary zone pre-mRNA are spatially indistinguishable by fluorescence microscopy (Fig. 2, *K–M* and *O–Q*).

Thus, the primary zone represents a high concentration of SgSLAC1 pre-mRNA at the locus of the SgSLAC1 gene. This locus consists of the many copies of the SgSLAC1 gene synapsed to make up a segment of the polytene chromosome axis. Consistent with this, primary zones have a thin disc shape with a diameter similar to a polytene chromosome arm (ca. 5 μm, Fig. 3).

SgSLAC1 Pre-mRNAs Are also Distributed throughout an Extrachromosomal Channel Network

In addition to concentration in the primary zone, SgSLAC1 pre-mRNAs are distributed in a network-like fashion throughout the extranucleolar nucleoplasm (see for example, Fig. 2, *A* and *B*). Confocal microscopy indicates that this network-like appearance results from optical section through signal distributed in thin sheets enclosing large, roughly cylindrical portions of the nucleoplasm (Fig. 3, see figure legend for important additional details).

These sheets comprise a network of interconnecting channels (Fig. 3). Evidence in a latter section indicates that the cylindrical, dark areas are polytene chromosome arms and that this channel network is defined by the simple process of exclusion from the chromosome arms, nucleolus, and nuclear surface. In spite of this apparent simplicity of organization, this network is centrally involved in subnuclear compartmentalization of pre-mRNA metabolism. We therefore refer to it explicitly as the extrachromosomal channel network (ECN).

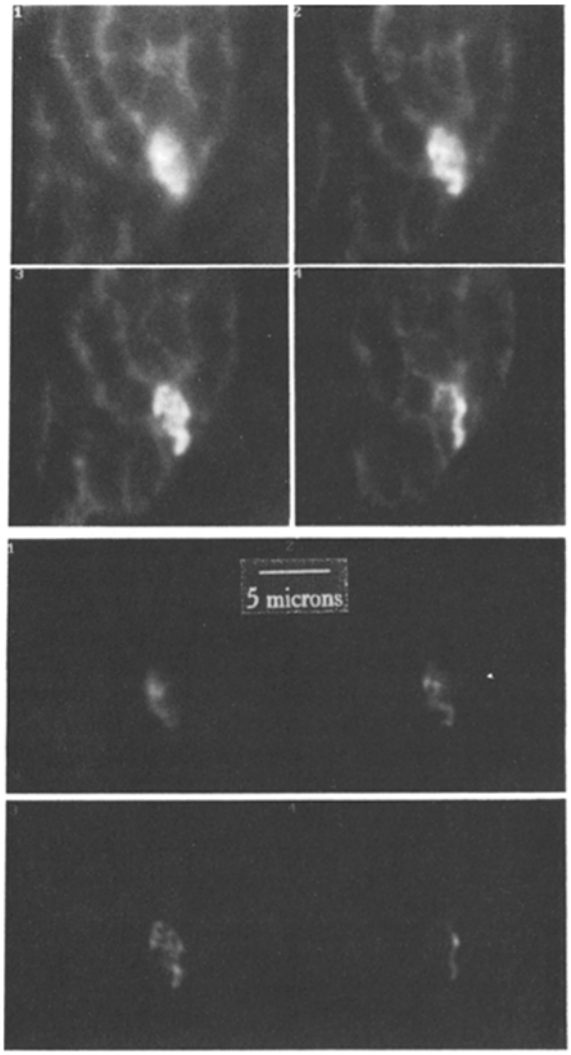

Figure 3. Confocal imaging of the nuclear distribution of SgSLAC1 pre-mRNA. Shown is a stack of four serial, nonoverlapping confocal optical sections (0.5 micron displacement between sections) through a salivary gland nucleus from an SgSLAC1-containing strain hybridized with the Lac probe in Fig. 1. The sections are numbered sequentially (*1–4*) and the top and bottom image sets are different photographic exposures. The primary zone (*text*) is visible in the lower right portion of each image. The sheetlike structure of the ECN (*text*) signal can be visualized in two ways. First, the primary zone is seen nearly broad side on—the axis of the chromosome containing it is slightly tilted from perpendicular to the plane of section. As a result, the primary zone is partially out of the plane in section #4 and a portion of the sheetlike ECN can be seen in cross section enwrapping the left margin of the chromosome. Second, most of the linelike features persist through all four sections as expected if they result from section through roughly vertical sheets. These results and evidence below indicate that the dark portions of the image are polytene chromosome arms contributing to formation of the ECN by exclusion.

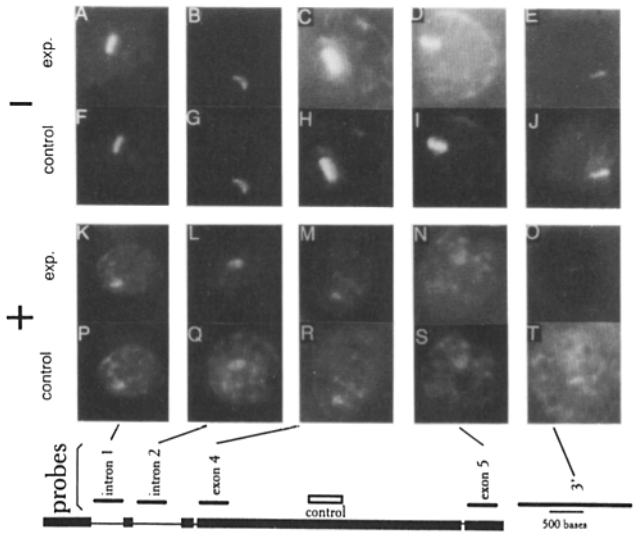

Figure 4. Detailed analysis of nuclear distribution of spliced and unspliced SgSLAC1 pre-mRNAs in the presence and absence of the *su(w^a)* splicing regulator. Shown are two rows of image pairs. Each image pair shows the result of a double-label in situ hybridization. One member of each pair (*control*; *F–J* and *P–T*) shows hybridization with the biotinylated control probe indicated in the diagram at bottom and the other (*exp.*; *A–E* and *K–O*) hybridization with the digoxygenylated experimental probe indicated by the lines connecting to diagram at bottom (see Materials and Methods for details). Probes were used at saturating inputs. The top row of image pairs (*A–J*) shows results in the absence of *su(w^a)* protein (in the g165 deletion allele background) and the bottom row (*K–T*) with the same probe set in the presence of the *su(w^a)* protein (wild-type genetic background). *A–J* have been overexposed to allow visualization of the relatively weaker ECN labeling in the absence of the *su(w^a)* protein (also see Fig. 1). As well, the experimental *E* and *O* were overexposed to show the weak primary zone signal.

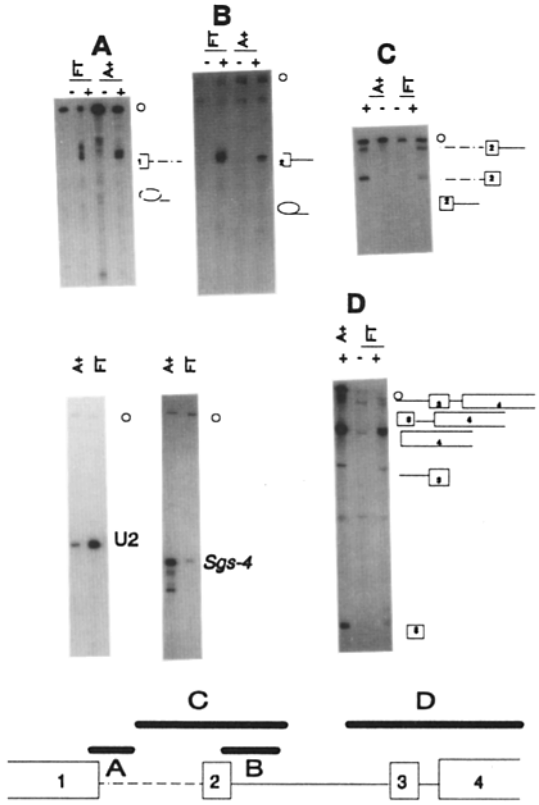

Figure 5. S_1 protection analysis of SgSLAC1 RNA products. (See Materials and Methods for details.) Diagrammed at the bottom in relation to the first four exons (boxes *1–4*) and first three introns of SgSLAC1 are the four S_1 protection probes used. In addition, each probe has an extension shifting its mobility upward relative to protection products. *A–D* show experiments with the corresponding probe. Positions of protection products corresponding to various spliced and unspliced SgSLAC1 RNAs are graphically indicated. − indicates the absence of the SgSLAC1 gene and + indicates its presence. All RNAs were made from individuals carrying the g165 deletion allele at the endogenous *su(w^a)* locus. FT and A+ indicate oligo-dT cellulose flow-through and bound RNA, respectively. (In the FT+ channel of *D* the bands are as follows, top to bottom: protector, second intron-second exon-third intron-fourth exon, protection product from *su(w^a)^{g165}* allele, fourth exon, second intron-third exon, protection product from *su(w^a)^{g165}* allele, and third exon.) Also shown are control experiments assessing enrichment for a polyadenylated mRNA (*Sgs-4*) and a nonpolyadenylated RNA (*U2 snRNA*) in the corresponding fractions. The position of undigested probe is indicated in all panels by a small circle. Note little or no product corresponding to splicing of the first intron before the second (*C*) or the second intron before the third (*D*). Small protection products corresponding to mature first or second exons are run off the gels in *A–C*. A small, GC-rich polylinker secondary structure in the A protector results in a low level of extension of the expected protection products by 3–10 bases (*A*; our unpublished results).

SgSLAC1 Pre-mRNA Shows Delayed Processing and the Extrachromosomal Channel Network RNA Population Is Incompletely Spliced, Polyadenylated Pre-mRNA

We focus here on SgSLAC1 pre-mRNA in the absence of the *su(w^a)* splicing repressor; effects of the repressor will be discussed in a subsequent section. Hybridization with probes for small regions of the gene allows definition of intranuclear distributions of intron and exon sequences (Fig. 4, *A–J*; note higher photographic exposure levels in absence of the regulator). Exon sequences are present in the primary zone and distributed throughout the ECN (Fig. 4, *C* and *D*).

Probes immediately 3′ to the SgSLAC1 polyadenylation site show no hybridization to ECN RNA (Fig. 4 *E*). Probes immediately 5′ to the polyadenylation site strongly label ECN RNAs (Fig. 4 *D*). These results define the 3′ ends of ECN RNAs thereby indicating that they are polyadenylated.

Hybridization with second intron probes shows a strong signal over the primary zone and very weak ECN labeling relative to exon probes (Fig. 4, *B* and *G*). S_1 protection experiments demonstrate that essentially all of this intron signal consists of unspliced pre-mRNA (steady state levels of excised intron are below detectability; Fig. 5 *B*). These results indicate that a large fraction of RNAs in the primary zone contain an unspliced second intron and are thus nascent or young transcripts. In contrast, the second intron has been removed from a larger proportion of the ECN RNA population indicating that these are older pre-mRNAs.

Splicing of the efficiently regulated first intron in the absence of the regulator shows an informative pattern. First, intron probes label both primary zone and ECN transcripts with comparable intensities relative to exon probes (Fig. 4

A). These first intron signals represent essentially entirely unspliced pre-mRNA rather than excised intron as assessed by S_1 protection (Fig. 5 *A*).

These results indicate that a large proportion of nascent (primary zone) SgSLAC1 transcripts contain first and second introns and that a similarly large proportion of ECN RNAs retain their first introns. S_1 protection experiments further corroborate this view. Specifically, ~30% of oligo-dT cellulose flow-through transcripts (enriched in nonpolyadenylated, nascent transcripts) retain their second introns (Fig. 5 *D*). Also, all of these plus an additional ~30% retain their first introns (Fig. 5 *C*). This corresponds to ~60% of presumptive nascent transcripts retaining the first intron. Moreover, this represents a minimal estimate as this nonpolyadenylated RNA fraction contains a small—but in this case, significant—contamination with polyadenylated RNAs (*Sgs-4* control, Fig. 5) that are highly enriched in fully spliced SgSLAC1 mRNAs (Fig. 1, *upper left*). Correcting for this contamination we estimate that ~50% of nascent transcripts retain their second introns and a very large fraction—approaching 100%—retain their first introns. Lastly, a small, but readily detectable, fraction of polyadenylated SgSLAC1 RNAs carry first and, to a lesser degree, second intron sequences (Fig. 5, *B–D*) as expected.

The stoichiometric ECN labeling by first intron probes (relative to exon probes; Fig. 4, *A* and *F*) indicates that there is relatively little fully spliced SgSLAC1 mRNA in the ECN. As the majority of total polyadenylated SgSLAC1 RNA at steady state is fully spliced under these conditions (Fig. 1, *upper left*) it follows that fully spliced SgSLAC1 mRNAs likely exit the nucleus significantly faster than incompletely spliced RNAs.

In summary, these results indicate that splicing of the first SgSLAC1 intron (and, to a lesser degree the second) is slow. The resulting incompletely spliced pre-mRNA is retained in the nucleus and is distributed throughout the ECN. In contrast, fully spliced SgSLAC1 mRNA is apparently relatively rapidly exported from the nucleus.

Unlike the first two regulated SgSLAC1 introns, the constitutive third intron is rapidly spliced. Specifically, no S_1 protection products are detected corresponding to removal of the second intron before the third whereas products resulting from removal of the third before the second are relatively abundant in nonpolyadenylated (nascent) RNAs (Fig. 5 *D*). The small portion of nascent transcripts retaining the third intron indicates that this intron is usually or always removed cotranscriptionally as has been observed previously for many constitutively spliced *Drosophila* introns (Osheim et al., 1985; Beyer and Osheim, 1988; Lemaire and Thummel, 1990).

Estimation of Rates of Movement of SgSLAC1 Pre-mRNAs through the ECN

Our results indicate that polyadenylated SgSLAC1 pre-mRNA moves away from the gene isotropically through the ECN. This suggests diffusion as the basis of this movement and predicts corresponding rates (Discussion). A useful estimate of the limits for these rates can be made as follows.

First, relative SgSLAC1 pre-mRNA residence times in the primary zone and ECN correspond to the relative amounts of RNAs in these two compartments assuming no large losses in moving from primary zone to ECN. The relative amounts of RNA in the primary zone and ECN can be estimated on the basis of S_1 protection as follows. A very large proportion of SgSLAC1 primary zone (nascent, nonpolyadenylated) and ECN (polyadenylated) transcripts retain their first introns as assessed by in situ hybridization (Fig. 4, *A* and *F*). Moreover, most or all incompletely spliced transcripts are likely in these two compartments. S_1 protection shows approximately equal amounts of first intron-containing transcripts in polyadenylated and nonpolyadenylated RNA preparations indicating approximately equal amounts of RNA in the ECN and primary zone, respectively (Fig. 5 *A*). Quantitation of fluorescent in situ hybridization signals yields similar estimates (results not shown).

Second, the absolute primary zone residence time for SgSLAC1 transcripts likely corresponds approximately to the time required to complete the 7.2-kb SgSLAC1 primary transcript (ca. 7 min; Thummel, 1992). It follows from the estimate of relative residence times in the preceding paragraph that the absolute, average ECN residence time (time to ECN loss) of incompletely spliced SgSLAC1 RNAs (in the absence of the *su(w^a)* regulator) is of the order of 7 min.

ECN SgSLAC1 pre-mRNAs achieve a uniform distribution during this residence time (see for example, Fig. 4, *F–J*). It follows that the mean time for a single transit of the ECN by SgSLAC1 pre-mRNA is substantially shorter than ca. 7 min.

Evidence that Most or All mRNAs Move from the Gene to the Nuclear Surface through the ECN

The route of movement of mature mRNAs from the gene to the nuclear surface is obscure. Incompletely spliced SgSLAC1 pre-mRNAs apparently move away from the gene by diffusion through the ECN (Discussion). As the ECN provides access to the nuclear surface, this is a likely route for intranuclear movement for mature mRNAs as well. The following study strongly supports this hypothesis.

Because of efficient export of mature mRNAs, diffusional intranuclear transport predicts steady state ECN levels of individual mature mRNAs too low to detect by currently available fluorescent in situ hybridization techniques (Discussion). The apparently low ECN level of fully spliced SgSLAC1 mRNA (above) is consistent with this expectation. Moreover, a second abundant nuclear pre-mRNA we have examined—one not showing the delayed processing of SgSLAC1—displays a primary zone but does not accumulate to detectable levels in the ECN (Fig. 6, *I–K*) as predicted.

Thus, the behavior of individual mature mRNAs are consistent with diffusional transport, but the limited sensitivity of available hybridization techniques does not allow individual mature mRNAs to be used to directly test this hypothesis. The following considerations allow a test. Most nuclear poly-A segments enter the cytoplasm (Jelinek et al., 1973; Latorre and Perry, 1973) indicating that most are components of mRNA precursors. Also, most intron removal in *Drosophila* is apparently cotranscriptional (Osheim et al., 1985; Beyer and Osheim, 1988; Lemaire and Thummel, 1990; above). Thus, a large fraction—possibly a large majority—of nuclear poly-A segments in *Drosophila* are likely to be mature mRNAs en route to export.

Thus, if mature mRNAs move from gene to nuclear surface by diffusion through the ECN, bulk poly-A should pre-

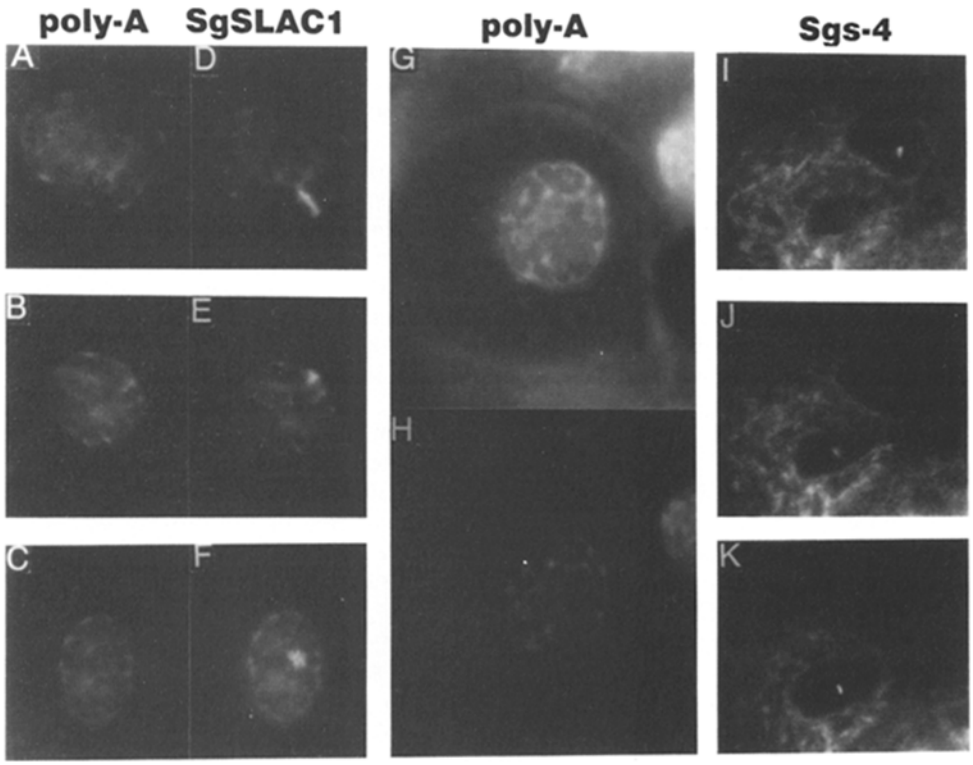

Figure 6. Evidence that most or all polyadenylated nuclear pre-mRNAs are distributed throughout the ECN. At left are double-label hybridizations to SgSLAC1 pre-mRNA (*Lac*; *D–F*) and bulk poly-A (poly-T probe; *A–C*). The primary zones are visible in *D–F* but are not detectably labeled in *A–C*. Note the near identity of the ECN labeling by the two probes in each image pair (*AD*, *BE*, and *CF*). *G* and *H* show hybridization to a wild-type strain (SgSLAC1 not present) with the poly-T probe. *G* shows a longer photographic exposure. At right is a stack of three serial, nonoverlapping confocal optical sections (one micron displacement) through a wild-type salivary gland hybridized with a probe for the *Sgs-4* mRNA. Note the presence of a primary zone but no detectable ECN labeling in each of the two nuclei shown. Also note the high cytoplasmic levels of this mRNA. (*Sgs-4* encodes a secreted protein and the "textured" appearance of the cytoplasmic signal may represent mRNA association with the ER.)

cisely colocalize with ECN SgSLAC1 pre-mRNA. This is observed in double-label hybridization experiments (Fig. 6, *A–F*).

The su(w^a) Splicing Regulator Inhibits Removal of Two SgSLAC1 Introns and Leads to Increased Accumulation of Unspliced Pre-mRNA in the ECN

su(w^a) protein provided in trans inhibits splicing of the first two SgSLAC1 introns and unspliced pre-mRNA accumulates (Fig. 1, *upper left*). Neither the amount of SgSLAC1 RNA in the primary zone (Fig. 1, *upper right*) nor the proportion of primary zone transcripts retaining first introns (Fig. 4, *A*, *F*, *K*, and *P*) is detectably altered by the regulator. This is expected from the observation that the first intron is not efficiently cotranscriptionally spliced even in the absence of the regulator (above).

In contrast, ECN levels of transcripts containing the efficiently regulated first intron increase substantially in the presence of the regulator (Fig. 1, *upper right*; Fig. 4, *A* and *K*—note different exposure levels for Fig. 4, *A* and *K*). Northern and S_1 protection analyses indicate that this elevated intron signal is due largely or entirely to unspliced introns (Fig. 1, *upper left* and results not shown).

We also observe a substantial increase in the ECN levels of regulated second intron-containing SgSLAC1 transcripts in the presence of the *su(w^a)* regulator (Fig. 4, *B* and *L*). Labeling of ECN SgSLAC1 RNA with second intron probes (relative to exon probes) is weaker than for first intron probes (Fig. 4, *K* and *L*) in agreement with Northern measurements (Fig. 1, *upper left*) indicating that only 30–50% of first intron-containing polyadenylated transcripts also retain the second intron in the presence of the *su(w^a)* protein.

These results have two direct implications. First, results described in preceding sections indicated that fully spliced mRNAs rapidly exit the nucleus while unspliced transcripts are retained in the ECN. The behavior of SgSLAC1 RNAs in the presence of the regulator strongly supports this interpretation. Second, the first SgSLAC1 intron is rarely or never removed cotranscriptionally (above) and repression of first intron splicing results in accumulation of unspliced RNA in the ECN. Collectively, these results suggest that removal of the regulated first intron may often or always occur in the ECN.

Evidence that snRNPs Are Concentrated in a Nuclear Subcompartment Consisting of the ECN and Polytene Interbands

The following study allows us to relate the organization of snRNPs to that of nuclear pre-mRNAs. We find extensive colocalization of these two classes of molecules in the ECN. Also, this study provides the clearest available spatial definition of the ECN.

We observe similar (presumably identical) nuclear label-

ing patterns with U2 snRNA probes and antibodies against the U2 snRNP-associated B″ epitope (see Fig. 8, *bottom panel*). Using these two probes we find that U2 is distributed throughout the space bounded, largely or entirely, by chromosome arms and nuclear surface (Fig. 7, *A* and *B*), and the nucleolus (Fig. 7, *E* and *F*). (See the legend to Fig. 7 for important additional details.) In addition to this ECN distribution, U2 is also found in discrete segments within chromosome axes (Fig. 7, *C* and *D*). In all cases where a determination is possible, these segments of chromosome-axis labeling are coextensive with the "interbands" characteristic of polytene chromosomes (Fig. 7, *A* and *B* and results not shown). (Polytene chromosome interbands represent relatively decondensed chromatin and contain most or all active genes [Ashburner, 1989 and references therein].) Future studies with improved techniques will be necessary to determine whether occasional exceptions to this pattern are seen. However, we will assume for simplicity here that this pattern accounts for all organization of the U2 signal.

Double-label hybridization with snRNA probes relates the other snRNAs to the U2 distribution (Fig. 8, *top panel*). The major features of the U2 pattern are very similar to the U1 pattern indicating that both snRNAs are distributed throughout the ECN. Moreover, the U4, U5, and U6 snRNAs are partially (but less completely) concentrated in the ECN.

Pre-mRNA/snRNA double-label hybridization relates the pre-mRNA and snRNP pattern. The ECN pre-mRNA distribution is very similar to the ECN portion of U2 distribution (Fig. 7, *E* and *F*). In contrast to U2, SgSLAC1 pre-mRNA apparently does not efficiently penetrate chromosome axes other than at its own primary zone (Fig. 7, *E* and *F*). Confinement of SgSLAC1 pre-mRNA to the ECN is further supported by a large number of conventional, epifluorescent images in which nuclear pre-mRNA (digoxygenin probes)

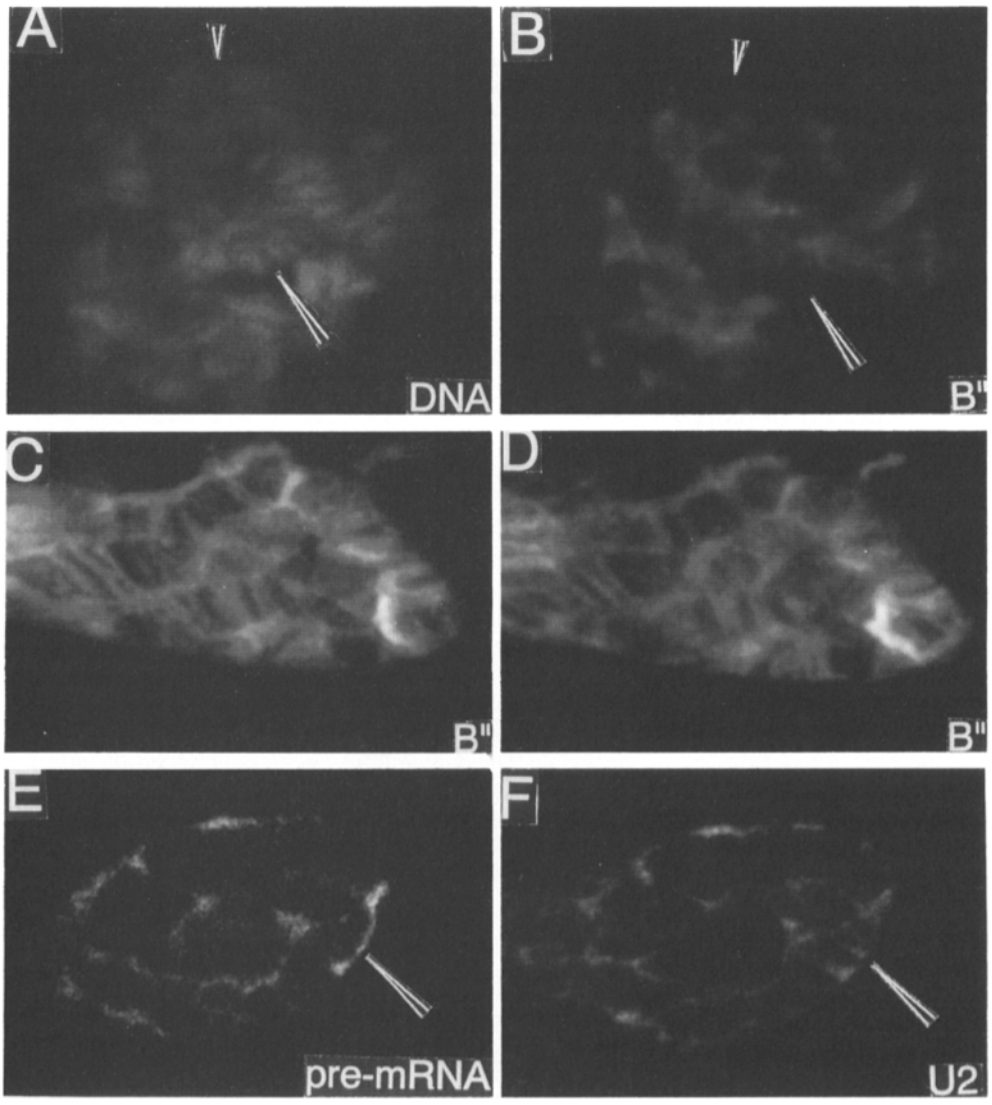

Figure 7. Confocal imaging of nuclear organization of U2 snRNPs and SgSLAC1 pre-mRNA. *A* and *B* show confocal sections through the same plane of a nucleus in which DNA and the *B″* U2 epitope, respectively, are labeled. The necessary RNase treatment (Materials and Methods) results in some loss of *B″* signal and detail. However, gross features of the pattern can be seen. Note that the chromosomal and *B″* patterns are often negative images of one another (begin at the small point at top and proceed downward). The *DNA* signal is generally weak in those regions where *B″* and *DNA* signals overlap. This is consistently observed and indicates that superposition often or always results from the optical sections being thick enough to include underlying (*overlying*) chromosomal material and overlying (*underlying*) *B″* signal. The large point shows an interband region corresponding to a region of *B″* labeling. *C* and *D* show two serial nonoverlapping optical sections (0.5 micron displacement) through a *B″* immunolabeled salivary gland nucleus. As neither RNase or protease treatment is required, these images likely represent the most faithful representation of the ECN (and connecting interbands) available. Negative images of polytene chromosome segments with characteristic cross striations (*interbands*) are clearly visible. *E* and *F* show confocal sections through the same plane of a nucleus labeled by hybridization to SgSLAC1 pre-mRNA (digoxygenylated) and U2 RNA (biotinylated), respectively. The patterns are largely superposable except for the cross striations (*point*) apparently representing entry into interbands by U2 but not by SgSLAC1 pre-mRNA (*text*). The SgSLAC1 primary zone is not subtended by this section. Note that both RNAs are largely or entirely excluded from the large central nucleolus visible in cross section in these images.

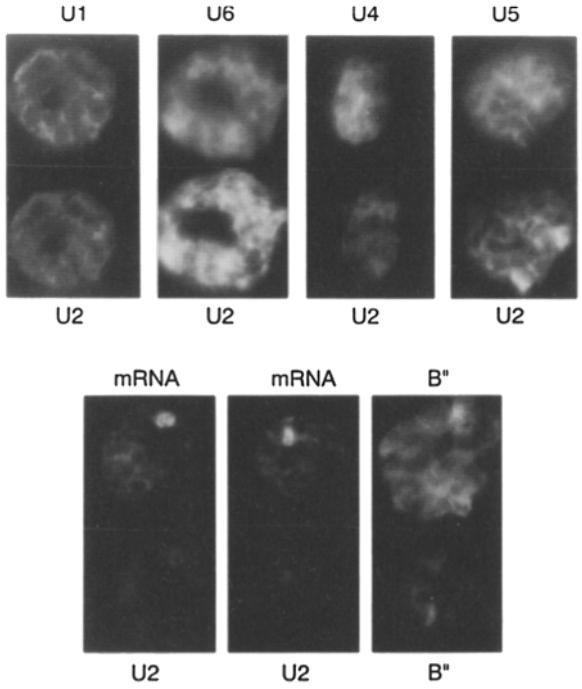

Figure 8. Epifluorescence imaging of polytene nuclear snRNP and SgSLAC1 pre-mRNA distributions. The top panel shows double-label hybridization with a U2 snRNA probe (biotinylated) and each of the other major, splicing-associated snRNAs (digoxygenylated) as indicated. The major features of the two patterns are substantially superposable. Note that U4, U5, and U6 show significant labeling throughout the extranucleolar nucleus in addition to concentration in the ECN. In the bottom panel, the left hand two image pairs show double-label hybridization to SgSLAC1 pre-mRNA (Lac; digoxygenylated) and U2 (biotinylated) snRNA. The networklike portions of the two signals are largely superposable. Also note that U2 snRNA concentrates to some degree over the very high level of transcripts produced in the SgSLAC1 primary zone. The rightmost portion of the bottom panel shows two nuclei immunolabeled with an antibody against the *B"* U2 snRNP epitope.

and chromosomal DNA (DAPI) are simultaneously labeled (results not shown).

Evidence that Diploid and Polytene Nuclei Show Similar Organization

The question arises as to whether nuclear pre-mRNA metabolism is organized differently in polytene and diploid nuclei. While differences in fundamental mechanism and organization are unlikely on first principles, they cannot be rigorously excluded.

To address this we compared distributions of splicing components in these two classes of nuclei (Fig. 9 and results not shown). We observe a striking similarity in the labeling patterns of diploid imaginal disc nuclei and polytene salivary gland nuclei. A network-like signal is distributed throughout the extranucleolar nucleoplasm with a very similar overall appearance and organization (scaled to nuclear volume) in each nuclear type.

Substantial additional analysis will be required to unambiguously determine whether these very similar labeling patterns actually result from fundamentally similar nuclear organization. However, these observations represent strong circumstantial evidence for similar organization.

Discussion

Organization of Nascent Transcripts

By far, the highest concentration of polytene nuclear pre-mRNAs occurs in the primary zone. Primary zone RNAs consist largely or entirely of nascent or very young pre-mRNAs. Primary zones often appear to contain limited, variable internal fiber-like substructures. However, double-label hybridization experiments indicate that this substructure results largely or entirely from organization of the underlying template DNA (Fig. 2, *M* and *Q*). High local template copy number in polytene nuclei permits use of short probe segments (500–3,400 bases). Thus, these apparently extended structures are generally too long to be single DNA molecules. Homologous genetic loci associate laterally in somatic *Drosophila* nuclei (by an unknown mechanism) as evidenced, for example, by the polytene chromosomes themselves. We suggest that this lateral association of template loci generates the limited appearance of primary zone substructure under our conditions.

Also, electron microscopic analysis of the giant *Chironomous* Balbiani ring transcription units in sectioned nuclei likewise reveals no long range organization of nascent transcripts other than that resulting from connection to template DNA (Stevens and Swift, 1966; Mehlin et al., 1992 and references therein).

Observations in various diploid mammalian cells reveal the highest nuclear pre-mRNA concentrations in fiber-like "tracks" (Lawrence et al., 1989; Huang and Spector, 1991; Xing and Lawrence, 1991). One particularly provocative interpretation of these observations is that some aspect of nuclear RNA metabolism or transport is organized around an extended, nonnucleic acid filament-like structure. This hypothesis is based on several observations suggesting that these nuclear tracks may not be simply "trees" of nascent transcripts organized around template DNA. However, we believe that none of these results is conclusive. The primary arguments and our critiques of them are as follows.

First, it is argued that tracks are too long to be organized around template DNA. However, the total length of the transcription unit (as opposed to the segment encoding the polyadenylated, mature mRNA species) is uncertain in all of these cases. Moreover, the most highly extended tracks were observed in nuclei that were swelled before hybridization (Lawrence et al., 1989). This may stretch template chromatin to or near B-form in length (ca. 3 kb per μm). Also, highly extended tracks were observed in the presence of two closely spaced copies of a potentially large transcription unit (ca. 18–30 kb or greater). Under these conditions the total length of the relevant transcription trees could approach 20 μm under conditions where a mean track length of 5 μm is observed (Lawrence et al., 1989).

Second, hybridization to template DNA in one case revealed small dot-like structures under conditions when hybridization to RNA displayed track-like signals (Lawrence et al., 1989). However, while hybridization to a high density of nascent RNA transcripts may reveal an entire transcription tree, hybridization to a single template DNA molecule

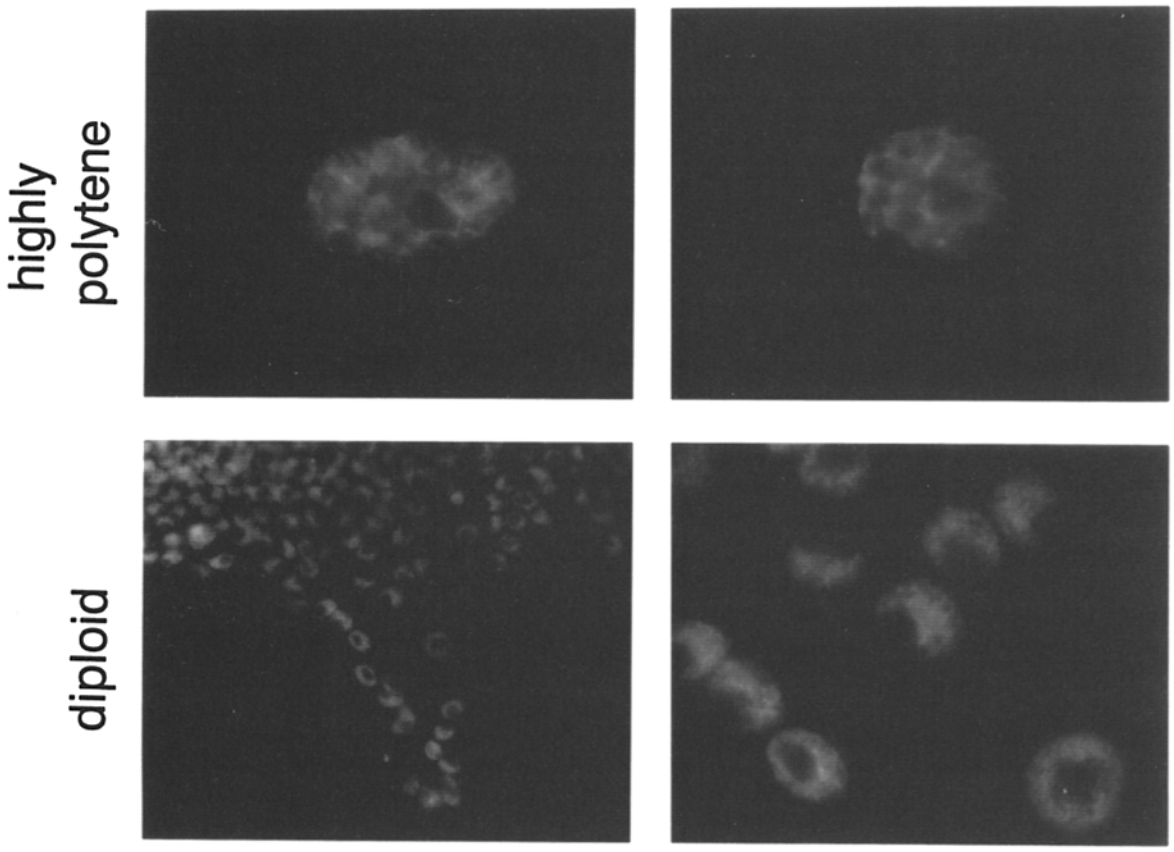

Figure 9. Evidence that U2 snRNA is organized similarly in diploid and polytene nuclei. All nuclei in the figure are from the same smear preparation hybridized with a probe for the U2 snRNA. The top panel shows two salivary gland nuclei. The bottom left panel shows a group of diploid imaginal disk nuclei at the same magnification as the polytene nuclei. The bottom right panel shows a portion of the diploid field photographically enlarged to near the same apparent diameter as the polytene nuclei.

may result in the relatively weak signal being visible above background only where the template molecule is tightly coiled or condensed to produce high local signal concentration. Extended portions of the template (including extended transcribing sequences) may not generate a detectable signal. Note that in our studies convenient detection of template DNA was made possible by the high local template copy number in polytene nuclei.

Lastly, in one case, nuclear tracks appeared to be resistant to DNase destruction of the template during nuclear "matrix" preparation suggesting the involvement of some additional structure (Xing and Lawrence, 1991; see below for further discussion of nuclear matrices). These results could be interpreted to indicate adventitious adhesion of nascent transcripts to the "matrix" during preparation. Under such conditions nascent transcript arrays would retain their spatial arrangement after destruction of the underlying DNA template. Furthermore, the possibility of selective retention of actively transcribing DNA segments (and their associated nascent transcripts) in matrix preparations (see for example, Jackson and Cook, 1988) is not excluded in these studies.

In summary, in our view, no conclusive evidence currently exists for organization of nuclear pre-mRNA around extended, nonnucleic acid filaments. We suggest that most or all track-like structures observed in mammalian nuclei represent nascent transcript "trees" organized around template DNA corresponding to the polytene primary zone.

Transport of Nuclear Pre-mRNA from Gene to Nuclear Surface

Our results indicate that pre-mRNAs move from the gene to the nuclear surface by diffusion through the ECN. First, the structure of the ECN indicates that it is a system of interconnected channels permitting diffusion between genes and the nuclear surface.

Second, movement of SgSLAC1 pre-mRNA from the gene through the ECN is isotropic as expected for diffusion.

Third, bulk polyadenylated nuclear RNA is distributed uniformly throughout the ECN strikingly similarly to SgSLAC1 pre-mRNA suggesting that most or all nuclear pre-mRNAs move by a common isotropic mechanism.

Fourth, early microinjection experiments with large, neutral, xenobiotic carbon particles (D'Angelo, 1946 and references therein) strongly suggest generalized diffusion of large particles between interchromosomal spaces and the nuclear surface.

Fifth, predicted in vivo diffusion rates for pre-mRNPs account for experimentally observed nuclear transit times. Fluorochrome-conjugated dextrans with radii of the order of

5 nm show apparent nuclear diffusion coefficients of ca. 3×10^{-8} (cm^2/s) (Peters, 1984). Radii of nuclear pre-mRNPs are ~10–25 nm (Beyer and Osheim, 1988; Dreyfus et al., 1988; LeStourgeon et al., 1991; Mehlin et al., 1992 and references therein) corresponding to predicted in vivo diffusion coefficients of $0.6–1.5 \times 10^{-8}$. The mean radius of salivary gland nuclei is ~15 μm (Fig. 3). This corresponds to an expected mean time for diffusional transit of the ECN of 25–62.5 s. (From the relation, $r^2 = 6Dt$, where D is the diffusion coefficient, r is distance, and t is time [see Berg, 1983, for a review of basic diffusion theory].) Consistent with this expectation, we estimate mean ECN transit times for SgSLAC1 pre-mRNAs of substantially <7 min (Results).

(Note that if mature mRNAs are efficiently exported on their first diffusional visit to the nuclear surface, we predict mean ECN residence times for mature RNAs of ca. 30–60 s. The ca. 7-min ECN residence time for incompletely spliced SgSLAC1 pre-mRNAs generates a weak fluorescent in situ hybridization signal [see for example, Fig. 1, *upper right* and Fig. 4, *F–J*.] Therefore, the ca. 30–60-s residence time for mature mRNAs on the diffusion model predicts steady state ECN levels too low to detect by fluorescent in situ hybridization to individual mature mRNAs as observed).

Lastly, in contrast to diffusion, active transport models generally suppose highly directed movement of pre-mRNA from gene to nuclear surface on fiber tracks (see Lawrence et al., 1989 and Huang and Spector, 1991 for discussion of these models). Such active transport would presumably involve fiber motors and individual motor molecules generally achieve rates of the order of 1 μm per s (Uyeda et al., 1991; Vallee, 1991; references therein). Our results allow evaluation of such models as follows. In the case of *Sgs-4* in Fig. 6 (*I–K*), the gene is separated from the nuclear surface by ~5 μm. Under these conditions, the motor-driven transit time of an *Sgs-4* mRNA to the nuclear surface should be ~5 s. The transcription time for the 0.7-kb *Sgs-4* transcription unit is ca. 40 s (Thummel, 1992). Therefore, at steady state, the amount of *Sgs-4* pre-mRNA in such a hypothetical export track should be ca. 12% of the amount in the *Sgs-4* primary zone. This level of pre-mRNA in a highly localized export track connecting the *Sgs-4* gene with the nuclear surface would be readily detectable. However, we have not observed such features among a large number of images.

Various general considerations also strongly support diffusional intranuclear transport over models involving active transport. For example, metazoan transcription times range from ~1 min to 1 h or more (Thummel, 1992). It is therefore unlikely to be necessary to move mRNAs from the gene to the nuclear surface more rapidly than diffusion-limited times of the order of 1 min.

With the possible exceptions listed in the following paragraph, all currently available results involving intranuclear pre-mRNA transport of which we are aware can, in principle, be explained on the basis of channeled diffusion.

We have not yet examined members of the minority class of mRNAs that behave as if they are exported from the nucleus vectorially (apically or basally; Davis and Ish-Horowicz, 1991). The observations of Huang and Spector (1991) potentially involve such vectoral export from mammalian nuclei. It will be important to determine if these mRNAs behave differently than the majority of isotropically exported mRNAs. We note, however, that these observations could be accommodated by a model in which intranuclear transport is diffusional by making any one of several additional structural or mechanistic assumptions (our unpublished results).

In conclusion, we emphasize that the alternative hypothesis that intranuclear pre-mRNA transport involves an active process that faithfully mimics diffusion cannot be rigorously excluded with currently available methodologies. However, our results represent a substantial, coherent body of evidence for diffusion.

Implications for Delayed and Regulated Splicing

Our results demonstrate that the efficiently regulatable first SgSLAC1 intron is very slowly spliced—often or always failing to be removed cotranscriptionally—resulting in unspliced, polyadenylated RNA moving away from the gene through the ECN independently of the presence of the *su(w^a)* splicing repressor.

These results have several general implications. First, a large body of evidence indicates that regulated splicing events often involve suboptimal splicing signals (see for example, Chou et al., 1987*b*; Smith and Nadal-Ginard, 1988; Bell et al., 1988; Chang and Sharp, 1989; Tian and Maniatis, 1992 and references therein) and slow execution in vivo (Nevins and Darnell, 1978; Amara et al., 1984; Danner and Leder, 1985; Sittler et al., 1986; Leff et al., 1987). Our results support the generality of this phenomenon.

Second, these results suggest that such slow splicing events can undergo execution remotely from the site of initial pre-mRNA synthesis. Among other things, this is consistent with the hypothesis that some regulated splicing events might occur in special circumstances—for example, in specialized nuclear substructures.

Third, the uniform distribution of unspliced SgSLAC1 pre-mRNA throughout the ECN with apparent access to the nuclear surface strongly suggests that retention of incompletely spliced RNAs (see LeGrain and Rosbash, 1989; Chang and Sharp, 1989; references therein) results from discrimination by the export machinery at the nuclear surface.

Implications for Kinetics of Nuclear Pre-mRNA Metabolism

First, snRNPs move through both the ECN and the decondensed chromatin making up the interbands. Thus snRNPs are predicted to have diffusional access to active genes (interbands).

Second, we estimate that the ECN represents, very roughly, 10% of the nuclear volume. Thus, coconcentration of pre-mRNA and splicing machinery in the ECN should accelerate rates of processing by at least roughly an order of magnitude.

Third, this organization apparently results in roughly tenfold coconcentration of ECN-localized components and the export-import machinery at the nuclear surface. This should substantially increase the rate of capture of pre-mRNPs by the export machinery.

Toward a General Model for the Organization of Metazoan Nuclear Pre-mRNA Metabolism

Our results indicate that polytene nuclear pre-mRNA metabolism is organized in an ECN and further suggest a similar organization in *Drosophila* diploid nuclei. The following considerations allow us to provisionally generalize this model to all metazoan nuclei.

The organization of splicing components in vertebrate nuclei has been extensively investigated. While studies in these complex, diploid nuclei have limited capacity to define precise relationships between chromosome arms, individual genes, pre-mRNAs, and other nuclear structures, some organizational features are clear. Mammalian splicing components are concentrated in regions of the nucleus outside of those containing most of the condensed chromatin and the nucleoli (Fakan and Puvion, 1980; Spector, 1990; Carter et al., 1991; references therein). Moreover, these snRNP-containing regions appear to form a generally interconnected reticulum in many cell types (Spector, 1990 and references therein). Also, there is evidence for colocalization of bulk polyadenylated RNA with at least some features of these snRNP-rich nuclear regions in mammalian nuclei (Carter et al., 1991). Lastly, there is strong evidence for channel-like spaces between chromosome axes in one diploid amphibian cell type (Hutchison and Weintraub, 1985).

On the basis of our results and of this evidence from vertebrate nuclei, we propose that pre-mRNA metabolism in all metazoan nuclei is organized in extrachromosomal channels precisely analogously to the simple arthropod nuclei described here. On this view, nuclei throughout metazoa will be largely or entirely distinguished by minor topological differences as follows. Relative nuclear dimensions indicate that diploid interphase chromatids are more linearly compacted than polytene chromosomes. We, thus, anticipate that blocks of condensed chromatin defining exclusion channels in diploid nuclei will involve, more predominantly, association between heterologous chromosome segments in contrast to the predominance of homologous association in polytene nuclei. Furthermore, relatively decondensed transcribing segments are more likely to project out of the smaller diploid chromosome axis (see for example, Hutchison and Weintraub, 1985) in contrast to lying partially within the larger polytene chromosome axis.

On this generalized view, the ECN will be largely or entirely identical to several topologically less well-defined features in mammalian nuclei – the "RNP reticulum" (for review see Fakan and Puvion, 1980; Spector, 1990) and the "poly-A domain" (Carter et al., 1991).

Additional Questions

The generalized model for organization of nuclear pre-mRNA metabolism proposed above raises a number of new questions. Examples and possible resolutions are as follows.

First is the basis of separation of chromosomes and nucleoli to maintain diffusion channels. Short filament-based gels in which oligomerization is triggered by some surface feature(s) of chromosomes and nucleoli would likely be effective. Evidence for a gel-like nucleoplasm exists (see for example, Clark and Merriam, 1977; D'Angelo, 1950 and references therein). Gels based on short actin filaments (Scheer et al., 1984 and references therein) are attractive candidates.

Second, as yet undefined structures in addition to chromosomes and nucleoli conceivably contribute to defining the ECN by exclusion. Future, higher resolution analyses will be necessary to address this issue.

Third is the significance of punctate nuclear substructures in which components of the splicing machinery concentrate (see for example, Spector, 1990; Fu and Maniatis, 1990; Wu et al., 1991; Li and Bingham, 1991). Such structures are conspicuous features of vertebrate nuclei and possibly similar, though less conspicuous, structures exist in the polytene ECN (our unpublished results). Coadhesion of monomeric molecules (diffusible in a gel-like nucleoplasm) to produce large aggregates (stationary in a gel) is a plausible model for the origin of these structures. The results of Li and Bingham (1991) and Zahler et al. (1992) are consistent with this possibility. On this hypothesis, many questions of detailed function for these structures would remain. However, we note that a hypothesis under which punctate structures are crystal-like and "feed" a saturated liquid phase for purposes of homeostasis in the face of variable rates of transcription is attractive on the models for nuclear organization proposed here.

Fourth is the significance of insoluble nuclear "matrix" structures defined by various extraction procedures (see for example, Schroder et al., 1987; Agutter, 1988; He et al., 1990; Cook, 1991). A nucleoplasmic gel (above) susceptible to condition-dependent alteration (stabilization, solubilization, contraction, or swelling) in which various molecules and aggregates are embedded by diffusion would account well for many such structures and for their behavior and variability. We emphasize that our model and results in no way exclude the existence of very long intranuclear protein filaments (see for example, He et al., 1990 and Cook, 1991); however, our results argue against a direct role for such filaments in intranuclear pre-mRNA transport.

Lastly, we note that nuclear pre-mRNP particles can spend significant fractions of their transit in reversible association with immobile nuclear components (for example, a nucleoplasmic gel) without detectably altering their fundamentally diffusional behavior.

We are grateful to a number of colleagues for important discussions. Among these are Hao Li, Erwin London, Stuart McLaughlin, Edwin Smith, Deborah Spikes, Carl Thummel, David Ish-Horowicz, Kalpana White, and David Williams. We are particularly grateful to Ann Beyer, Stan Fakan, Paul Fisher, David Spector, and Gary Zieve for numerous, thoughtful discussions of specialized aspects of nuclear structure. We thank Dr. Cynara Ko of Jackson ImmunoResearch for making the antibiotin antibodies available to us.

This work was supported by National Institutes of Health grant GM32003 to P. M. Bingham.

Received for publication 25 November 1992 and in revised form 25 February 1993.

References

Agutter, P. S. 1988. Nucleo-cytoplasmic transport of mRNA: its relationship to RNA metabolism, subcellular structure and other nucleocytoplasmic exchanges. *Prog. Mol. Subcell. Biol.* 10:15–96.

Amara, S. G., R. M. Evans, and M. G. Rosenfeld. 1984. Calcitonin/calcitonin gene-related peptide transcription unit: tissue-specific expression involved selective use of alternative polyadenylation signals. *Mol. Cell. Biol.* 4:2151–2160.

Ashburner, M. 1989. Drosophila: A Laboratory Handbook. Cold Spring Harbor Laboratory Press, Cold Spring Harbor, NY. 33–42.

Baker, B. S. 1989. Sex in flies: the splice of life. *Nature (Lond.).* 340:521–524.

Bell, L. R., E. M. Maine, P. Schedl, and T. W. Cline. 1988. *Sex-lethal*, a Drosophila sex determination switch gene, exhibits sex-specific RNA splicing and sequence similarity to RNA binding proteins. *Cell.* 55:1037–1046.

Berg, H. C. 1983. Random walks in biology. Princeton University Press, Princeton, NJ. 1–138.

Beyer, A., and Y. Osheim. 1988. Splice site selection, rate of splicing and alternative splicing on nascent transcripts. *Genes & Dev.* 2:754–765.

Bingham, P. M., T.-B. Chou, I. Mims, and Z. Zachar. 1988. On/off regulation of gene expression at the level of splicing. *Trends Genet.* 4:134–138.

Carmo-Fonseca, M., D. Tollervey, R. Pepperkok, S. M. L. Baragino, A. Merdes, C. Brunner, P. Zamore, M. R. Green, E. Hurt, and A. I. Lamond.

1991. Mammalian nuclei contain foci which are highly enriched in components of the pre-mRNA splicing machinery. *EMBO (Eur. Mol. Biol. Organ.) J.* 10:195–206.

Carter, K. C., K. L. Taneja, and J. B. Lawrence. 1991. Discrete nuclear domains of poly(A) RNA and their relationship to the functional organization of the nucleus. *J. Cell Biol.* 115:1191–1202.

Chang, D. D., and P. A. Sharp. 1989. Regulation of HIV *rev* depends upon recognition of splice sites. *Cell.* 59:789–795.

Chou, T.-B., I. P. Mims, M. Belanich, Z. Zachar, and P. M. Bingham. 1987*a*. Procedural improvements in injections for P-mediated germline gene transfer. *Dros. Inf. Serv.* 66:156–157.

Chou, T.-B., Z. Zachar, and P. M. Bingham. 1987*b*. Developmental expression of a regulatory gene is programmed at the level of splicing. *EMBO (Eur. Mol. Biol. Organ.) J.* 6:4095–4104.

Clark, T. G., and R. W. Merriam. 1977. Diffusible and bound actin in nuclei of *Xenopus laevis* oocytes. *Cell.* 12:883–891.

Cook. P. R. 1991. The nucleoskeleton and the topology of replication. *Cell.* 66:627–635.

Cox, K. H., D. V. DeLeon, L. M. Angerer, and R. C. Angerer. 1984. Detection of mRNAs in sea urchin embryos by *in situ* hybridization using asymmetric RNA probes. *Dev. Biol.* 101:485–502.

Danner, D., and P. Leder. 1985. Role of an mRNA cleavage/poly(A) addition site in the production of membrane-bound and secreted IgM mRNA. *Proc. Natl. Acad. Sci. USA.* 82:8658–8662.

D'Angelo, E. G. 1946. Micrurgical studies on Chironomous salivary gland chromosomes. *Biol. Bull.* 90:71–87.

D'Angelo, E. G. 1950. Salivary gland chromosomes. *Ann. NY. Acad. Sci.* 50:910–919.

Davis, I., and D. Ish-Horowicz. 1991. Apical localization of pair-rule transcripts requires 3' sequences and limits protein diffusion in the *Drosophila* blastoderm embryo. *Cell.* 67:927–940.

Dreyfuss, G., M. S. Swanson, and S. Pinol-Roma. 1988. Heterogenous nuclear ribonucleoprotein complexes and the pathway of messenger RNA synthesis. *Trends Biochem. Sci.* 13:86–91.

Fakan, S., and E. Puvion. 1980. The ultrastructural visualization of nucleolar and extranucleolar RNA synthesis and distribution. *Int. Rev. Cytol.* 65:255–299.

Foe, V. E., and B. M. Alberts. 1985. Reversible chromosome condensation induced in *Drosophila* embryos by anoxia: visualization of interphase nuclear organization. *J. Cell Biol.* 100:1623–1636.

Fu, X.-D., and T. Maniatis. 1990. Factor required for mammalian spliceosome assembly is localized to discrete regions in the nucleus. *Nature (Lond.).* 343:437–441.

Hafen, E., and Levine, M. 1986. The localization of RNAs in *Drosophila* tissue sections by *in situ* hybridization. In *Drosophila*: A Practical Approach. D. B. Roberts, editor. IRL Press, Oxford, UK. 139–158.

He, D., J. A. Nickerson, and S. Penman. 1991. Core filaments of the nuclear matrix. *J. Cell Biol.* 110:569–580.

Huang, S., and D. L. Spector. 1991. Nascent pre-mRNA transcripts are associated with nuclear region enriched in splicing factors. *Genes & Dev.* 5:2288–2302.

Hutchison, N., and H. Weintraub. 1985. Localization of DNase I-sensitive sequences to specific regions of the interphase nuclei. *Cell.* 43:471–482.

Jackson, D. A., and P. R. Cook. 1988. Visualization of a filamentous nucleoskeleton with a 23nm axial repeat. *EMBO (Eur. Mol. Biol. Organ.) J.* 7:3667–3677.

Jelinek, W., A. Adesnik, M. Salditt, D. Sheiness, R. Wall, G. Molloy, L. Philipson, and J. E. Darnell. 1973. *J. Mol. Biol.* 75:515–532.

Kopczynski, C. C., and M. A. T. Muskavitch. 1992. Introns excised from the delta primary transcript are localized near sites of *Delta* transcription. *J. Cell Biol.* 119:503–512.

Krieg, P. A., and D. A. Melton. 1987. In vitro RNA synthesis with SP6 RNA polymerase. *Methods Enzymol.* 155:397–415.

Latorre, J., and R. P. Perry. 1973. The relationship between polyadenylated heterogenous nuclear RNA and messenger RNA: studies with actinomycin D and cordycepin. *Biochim. Biophys. Acta.* 335:93–101.

Lawrence, J. B., R. H. Singer, and L. M. Marselle. 1989. Highly localized tracks of specific transcripts within interphase nuclei visualized by *in situ* hybridization. *Cell.* 57:493–502.

Leff, S. E., R. M. Evans, and M. G. Rosenfeld. 1987. Splice commitment dictates neuron-specific alternative RNA processing in calcitonin/CGRP gene expression. *Cell.* 48:517–524.

Legrain, P., and M. Rosbash. 1989. Some cis- and trans-acting mutants for splicing target pre-mRNA to the cytoplasm. *Cell.* 57:573–583.

LeMaire, M. F., and C. S. Thummel. 1990. Splicing precedes polyadenylation during *Drosophila* E74A transcription. *Mol. Cell. Biol.* 10:6059–6063.

Lerner, E. A., M. R. Lerner, C. A. Janeway, and J. A. Steitz. 1981. Monoclonal antibodies to nucleic acid-containing cellular constituents: probes for molecular biology and autoimmune disease. *Proc. Natl. Acad. Sci. USA.* 78:2737–2741.

LeStourgeon, W. M., S. F. Barnett, and S. J. Northington. 1991. Tetramers of the core proteins of 40S nuclear ribonucleoprotein particles assemble to package nascent transcripts into a repeating array of regular particles. *In* The Eukaryotic Nucleus: Molecular Biochemistry and Macromolecular Assemblies. P. R. Strauss and S. H. Wilson, editors. Academic Press, New York. 470–502.

Li, H., and P. M. Bingham. 1991. Arginine/serine-rich domains of the *su(w^a)* and *tra* RNA processing regulators target proteins to a subnuclear compartment implicated in splicing. *Cell.* 67:335–342.

Lindsley, D. L., and G. G. Zimm. 1992. The Genome of *Drosophila melanogaster.* Academic Press, San Diego, CA. 1–1133.

Maniatis, T. 1991. Mechanisms of alternative pre-mRNA splicing. *Science (Wash. DC).* 251:33–34.

Maniatis, T., E. F. Fritsch, and J. Sambrook. 1982. Molecular Cloning: A Laboratory Manual. Cold Spring Harbor Laboratory Press, Cold Spring Harbor, NY. 545 pp.

McConnell, M., A. M. Whalen, D. E. Smith, and P. A. Fisher. 1987. Heat shock-induced changes in the structural stability of proteinaceous karyoskeletal element *in vitro* and morphological effects *in situ*. *J. Cell Biol.* 105: 1087–1098.

McNabb, S. L., and S. K. Beckendorf. 1986. Cis-acting sequences which regulate expression of the *Sgs-4* glue protein gene of *Drosophila*. *EMBO (Eur. Mol. Biol. Organ.) J.* 5:2331–2340.

Mehlin, H., B. Daneholt, and U. Skoglund. 1992. Translocation of a specific premessenger ribonucleoprotein particle through the nuclear pore studied with electron microscope tomography. *Cell.* 69:605–613.

Nevins, J. R., and J. E. Darnell. 1978. Steps in the processing of Ad2 mRNA: poly(A)+ nuclear sequences are conserved and poly(A) addition precedes splicing. *Cell.* 15:1477–1493.

Osheim, Y., O. L. Miller, and A. Beyer. 1985. RNP particles and splice junction sequences in *Drosophila* chorion transcripts. *Cell.* 43:143–151.

Peters, R. 1984. Nucleo-cytoplasmic flux and intracellular mobility in single hepatocytes measured by fluorescence microphotolysis. *EMBO (Eur. Mol. Biol. Organ.) J.* 3:1831–1836.

Puissant, C., and L. Houdebine. 1990. An improvement of the single-step method of RNA isolation by acid guanidinium thiocyanate-phenol-chloroform extraction. *Biotechniques.* 8:148–149.

Rubin, G. M., and A. C. Spradling. 1983. Vectors for P element-mediated gene transfer in *Drosophila*. *Nucleic Acids Res.* 11:6341–6351.

Scheer, U., H. Hinssen, W. W. Franke, and B. M. Jochusch. 1984. Microinjection of actin-binding proteins and actin antibodies demonstrates involvement of nuclear actin in transcription of lampbrush chromosomes. *Cell.* 39:111–122.

Schroder, H. C., D. Trolltsch, U. Friese, M. Bachmann, and W. E. G. Muller. 1987. Mature mRNA is selectively released from the nuclear matrix by an ATP/dATP-dependent mechanism sensitive to topoisomerase inhibitors. *J. Biol. Chem.* 262:8917–8925.

Shermoen, A. W., and P. H. O'Farrell. 1991. Progression of the cell cycle through mitosis leads to abortion of nascent transcripts. *Cell.* 67:303–310.

Sittler, A., H. Gallinaro, and M. Jacob. 1986. In vivo splicing of the pre-mRNAS from early region 3 of adenovirus-2: the products of cleavage at the 5' splice site of the common intron. *Nucleic Acids Res.* 14:1187–1207.

Smith, C. W. J., and B. Nadal-Ginard. 1989. Mutually exclusive splicing of alpha-tropomyosine exons enforced by an unusual lariat branchpoint location: implications for constitutive splicing. *Cell.* 56:749–758.

Spector, D. 1990. Higher order nuclear organization: three-dimensional distribution of small nuclear ribonucleoprotein particles. *Proc. Natl. Acad. Sci. USA.* 87:147–151.

Spikes, D., and P. M. Bingham. 1992. Analysis of spliceosome assembly and the structure of a regulated intron in *Drosophila in vitro* splicing extracts. *Nucleic Acids Res.* 20:5719–5727.

Springer, J. E., E. Robbins, B. J. Gwag, M. E. Lewis, and F. Baldino. 1991. Non-radioactive detection of nerve growth factor receptor (NGRF) mRNA in rat brain using *in situ* hybridization histochemistry. *J. Histochem. Cytochem.* 39:231–234.

Stevens, B. J., and H. Swift. 1966. RNA transport from nuclear to cytoplasm in Chironomous salivary glands. *J. Cell Biol.* 31:55–77.

Thummel, C. S., A. M. Boulet, and H. D. Lipshitz. 1988. Vectors for *Drosophila* P-element-mediated transformation and tissue culture transfection. *Gene (Amst.).* 74:445–456.

Thummel, C. S. 1992. Mechanisms of transcriptional timing in *Drosophila*. *Science (Wash. DC).* 255:39–40.

Tian, M., and T. Maniatis. 1992. Positive control of pre-mRNA splicing in vitro. *Science (Wash. DC).* 256:237–240.

Uyeda, T. Q. P., H. M. Warrick, S. J. Kron, and J. A. Sudich. 1991. Quantized velocities at low myosin densities in an *in vitro* motility assay. *Nature (Lond.).* 352:307–311.

Vallee, R. 1991. Cytoplasmic dynein: advances in microtubule-based motility. *Trends Cell Biol.* 1:25–29.

Wu, A., C. Murphy, H. G. Callan, and J. G. Gall. 1991. Small nuclear ribonucleoproteins and heterogeneous nuclear ribonucleoproteins in the amphibian germinal vesicle: loops, spheres and snurposomes. *J. Cell Biol.* 113:465–483.

Xing, Y., and J. B. Lawrence. 1991. Preservation of *in vivo* RNA distribution within the nuclear matrix demonstrated by *in situ* hybridization coupled with biochemical fractionation. *J. Cell Biol.* 112:1055–1064.

Zachar, Z., T.-B. Chou, and P. M. Bingham. 1987. Evidence that a regulatory gene autoregulates splicing of its transcript. *EMBO (Eur. Mol. Biol. Organ.) J.* 6:4105–4111.

Zahler, A. M., W. S. Lane, J. A. Stolk, and M. B. Roth. 1992. SR proteins: a conserved family of pre-mRNA splicing factors. *Genes & Dev.* 6:837–847.